Confocal Microscopic Analysis of the Interaction between Cisplatin and the Copper Transporter ATP7B in Human Ovarian Carcinoma Cells

Kuniyuki Katano, Roohangiz Safaei, Goli Samimi, Alison Holzer, Mika Tomioka, Murray Goodman, and Stephen B. Howell

Departments of Medicine, Chemistry and the Cancer Center, University of California, San Diego, La Jolla, California

ABSTRACT

Some cisplatin (DDP)-resistant cells overexpress the copper export transporter ATP7B, and cells molecularly engineered to overexpress ATP7B are resistant to DDP. The interaction of Cu with ATP7B normally triggers its relocalization from the perinuclear region to more peripheral vesicles. To investigate the interaction of DDP with ATP7B, we examined the effect of DDP on the subcellular localization of ATP7B using human ovarian carcinoma cells expressing a cyan fluorescent protein (ECFP)-tagged ATP7B (2008/ECFP-ATP7B). ATP7B expression was confirmed in 2008/ECFP-ATP7B cells by Western blotting, and its functionality was documented by showing that it rendered the cells 1.9-fold resistant to $CuSO_4$ and 4.1-fold resistant to DDP and also reduced the accumulation of both drugs. There was greater sequestration of Pt into intracellular vesicles in the 2008/ECFP-ATP7B cells than in the 2008/ECFP cells. Confocal digital microscopy revealed that ECFP-ATP7B localized in the perinuclear region in absence of drug exposure and that both Cu and DDP triggered relocalization to more peripheral vesicular structures. A fluorescein-labeled form of DDP that retained cytotoxicity and was subject to the same mechanisms of resistance as DDP colocalized with ECFP-ATP7B in the 2008/ECFP-ATP7B cells, whereas the same fluorochrome lacking the DDP moiety did not. These results provide evidence that DDP directly interacts with ATP7B to trigger its relocalization and that ATP7B mediates resistance to DDP by sequestering it into vesicles of the secretory pathway for export from the cell.

Received 12/12/03; revised 2/27/04; accepted 3/10/04.

Grant support: NIH Grants CA78648 and CA95298. This work was conducted in part by the Clayton Foundation for Research–California Division.

The costs of publication of this article were defrayed in part by the payment of page charges. This article must therefore be hereby marked *advertisement* in accordance with 18 U.S.C. Section 1734 solely to indicate this fact.

Note: R. Safaei and S. Howell are Clayton Foundation Investigators.

Requests for reprints: Stephen B. Howell, Department of Medicine 0058, University of California, San Diego, 9500 Gilman Drive, La Jolla, CA 92093-0058. Phone: (858) 822-1110; Fax: (858) 822-1111; E-mail: showell@ucsd.edu.

INTRODUCTION

Although many mechanisms may contribute to resistance to cisplatin (DDP; Refs. 1–3), reduced DDP accumulation is the single most consistently identified feature of cells with acquired DDP resistance both *in vitro* and *in vivo* (4–8). How DDP enters and exits from malignant cells remains poorly defined. Evidence suggesting that DDP uptake is mediated by a transporter mechanism or channel was published some time ago (9–14), and overexpression of glutathione GS-X pump has been reported in some DDP-resistant cell lines (15, 16). More recent studies have suggested that transporters that mediate Cu homeostasis also regulate the cellular pharmacology of DDP. Cells selected for DDP-resistance are cross-resistant to Cu, and cells selected for resistance to Cu are cross-resistant to DDP (17). A direct link between Cu transport and DDP resistance was identified by Komatsu *et al.* (18) who found that prostate cancer cells selected for resistance to DDP expressed increased levels of ATP7B and that cells transfected with ATP7B were resistant to both Cu and DDP.

ATP7B is responsible for the export of Cu from the liver, and mutations that disable the function of ATP7B cause Wilson's disease (19–21). ATP7B is believed to sequester Cu from cytoplasmic chaperones into the *trans*-Golgi network, where it is loaded onto ceruloplasmin and other Cu-requiring enzymes and subsequently exported from the cell via the vesicular secretory pathway (reviewed in Ref. 22). When environmental Cu levels are raised, ATP7B undergoes relocalization from the *trans*-Golgi network to vesicular structures whose exact nature has not been completely defined but which are believed to be part of the vesicular export pathway (23–27).

We have recently reported that some ovarian carcinoma cell lines selected for resistance to DDP overexpress ATP7B and that increasing the expression of ATP7B in human ovarian carcinoma cells renders them resistant to this drug (28). In the current study, we sought to additionally define the mechanism by which ATP7B mediates DDP resistance. We report here that, as with Cu, DDP triggers relocalization of ATP7B from the *trans*-Golgi network to vesicular structures and that a fluorescein-labeled form of DDP becomes concentrated into ATP7B-containing vesicles. These observations are consistent with the concept that DDP is a substrate for this Cu transporter and leaves the cell largely via the same vesicular export system as Cu.

MATERIALS AND METHODS

Drugs and Reagents. Cupric sulfate, carboplatin, and other chemicals were obtained from Sigma Co. (St. Louis, MO) and Fisher Scientific Co. (Tustin, CA). DDP (PLATINOL-AQ) was a gift from Bristol Laboratories (Princeton, NJ). The rabbit polyclonal anti-ATP7B antiserum was generously provided by

Dr. Jonathan D. Gitlin of Washington University (St. Louis, MO). Polyclonal antibody against actin was from Santa Cruz Biotechnology, Inc. (Santa Cruz, CA). Secondary antibodies were purchased from Amersham Biosciences (Piscataway, NJ). Bio-Rad Co. (Richmond, CA) supplied the Protein Assay kit used to measure protein concentration and the reagents for Western blotting. ^{64}Cu was purchased from the Mallinkrodt Institute (St. Louis, MO). Alexa Fluor 647-conjugated phalloidin and other reagents for microscopy were purchased from Molecular Probes (Eugene, OR).

DNA Cloning and Transfection. The human ovarian carcinoma 2008 cell line (29) and its variant sublines were grown in drug-free RPMI 1640 plus 10% FCS and maintained in humidified air containing 5% CO_2 at 37°C. A full-length ATP7B cDNA cloned into the pRC/CMV vector (pRc/CMV-ATP7B) and expressing a Geneticin resistance marker was generously provided by Dr. Toshihiro Sugiyama, and its details have been published elsewhere (30, 31). To produce the ECFP-ATP7B expression construct, the *Xba*I-*Afe*I fragment of the ATP7B cDNA (nucleotides 141-4488 of U11700 of the GenBank) was blunt ended at the *Afe*I site and cloned into the *Nhe*I-*Sma*I site of the pECFP-N1 vector (BD Biosciences Clontech, Palo Alto, CA). Cells were transfected with insert-containing or empty vectors with LipofectAMINE (Life Technologies, Inc., Grand Island, NY) according to the manufacturer's directions. Transfected cells were selected in the presence of 500 μg/ml Geneticin, and all surviving clones were combined to obtain a multiclonal population. The 2008/ATP7B cells were additionally engineered to express green fluorescent protein (GFP) by infecting them with the amphotrophic pMSCV-EGFP-puro retrovirus (32, 33) generously provided by Dr. Martin Haas. Seven days after transfection with the viral GFP-expressing vector, cells were subjected to fluorescence-activated cell sorting, and the 5% of the population with the brightest green fluorescence was selected and grown to mass culture in medium containing 500 μg/ml Geneticin and/or 1 μg/ml puromycin.

Synthesis of Fluorescein-Labeled Form of DDP (F-DDP) and cyclohexylmethylamido fluorescein (CHF). F-DDP was prepared using a modification of the method reported by Molennar *et al.* (34). Briefly, N^3-*t*Boc-1,2,3-propanetriamine was prepared from 3-amino-1,2-propanediol and then reacted with potassium tetrachloroplatinate to obtain [1-(*t*Boc-aminomethyl)-1,2-ehtylenediamine] dichloroplatinum(II). The *t*Boc group was removed in with 0.1 N HCl at 70°C, and the resulting platinated salt was neutralized with 2 N NaOH and then reacted with 5(6)-carboxyfluorescein preactivated by treatment with 1-ethyl-3-(3-dimethulaminopropyl)carbodiimide hydrochloride (EDAC) and *N*-hydroxysuccinimide in dimethylformamide. After centrifugation and successively washing with water, ethanol, and ether, the final product was characterized for DDP and fluorescein content by ^{1}H NMR and mass spectrometry.

Assays of Drug Sensitivity. Colony-forming assays were performed using triplicate cultures of 200 cells/35-mm plate grown in 5 ml of medium containing different concentrations of DDP, $CuSO_4$, F-DDP, or CHF until visible colonies had formed (10–14 days).

The dishes were rinsed twice with PBS, fixed with 100% methanol, and stained with a 0.1% crystal violet solution. A ChemiImager 4400 instrument (Alpha Inotech, San Leandro, CA) was used for counting colonies of >50 cells. Enrichment assays were performed by preparing a population containing 10% 2008/ATP7B-GFP cells and 90% 2008/EV cells, seeding 10^5 cells into 100-mm culture dishes, incubating them together for 24 h, and then exposing them to graded concentrations of drug for 1 h. Fresh nondrug-containing medium was then added, and the cells were grown for 5 days before being harvested by trypsinization and analyzed for the percentage of 2008/ATP7B-GFP cells in the surviving population by flow cytometry. Each assay was performed with triplicate cultures.

Cellular Pharmacokinetic Assays. Uptake measurements of ^{64}Cu were made using 35-mm dishes seeded with 10^6 cells each and incubated in medium until they were 75–80% confluent. For cellular accumulation experiments, the medium was replaced by 1 ml of fresh medium containing 2 μM $^{64}CuSO_4$, and the cells were incubated at 37°C. This Cu concentration was selected based on prior reports indicating that alterations in the cellular pharmacokinetic parameters could be detected at these concentrations (35, 36). At the requisite time points, the medium was poured off, and the dishes were quickly rinsed three times with ice-cold PBS, after which, the cells were scraped and transferred to scintillation vials containing 3 ml of scintillation solution (National Diagnostics, Atlanta, GA), and ^{64}Cu was quantified using a gamma counter. Six separate dishes were used for each time point in each experiment. Measurement of DDP accumulation in cells was made using 35-mm dishes seeded with 10^6 cells each and incubated in medium until they were 75–80% confluent. The medium was replaced by 1 ml of fresh medium containing 2 μM DDP, and the cells were incubated at 37°C. At the requisite time points in experiments, the medium was poured off, and the dishes were quickly rinsed three times with ice-cold PBS, after which, the cells were exposed to 215 μl of 70% nitric acid for 10 min. The cells were transferred into tubes and dissolved at 65°C for 2 h, after which, the samples were diluted with water to a final concentration of 5% acid. Indium atomic absorption standard solution (Acros Organics, Tustin, CA) was added to each sample at 1 ppb as a control for flow variation. Measurements were made using a Thermo Finnigan inductively coupled plasma mass spectrometer (model Element 2) from the Analytical Facility at the Scripps Institute of Oceanography. In all experiments, cells harvested from a separate group of six dishes were used to measure protein content by the Bradford assay. Uptake measurements of F-DDP were performed using 100-mm dishes seeded with 10^6 cells each and incubated in medium until they were 75–80% confluent. The medium was replaced with 10 ml of fresh medium containing 2 μM F-DDP, and the cells were incubated at 37°C. At the requisite time points, the medium was poured off, and the dishes were quickly rinsed three times with PBS, harvested by trypsinization, and analyzed for the percentage of fluorescent cells by flow cytometry. Each assay was performed with triplicate cultures.

Vesicle Preparations. Cells were plated in 145-mm plates and grown to ~80% confluency. Cells were exposed to 2 μM DDP for 24 h. All subsequent steps were performed with ice-cold solutions, and all centrifugation steps were performed at 4°C. The cells were rinsed once with PBS and then rinsed twice with 1 mM sodium bicarbonate solution. Each plate was then scraped with 1 mM sodium bicarbonate solution containing one Complete Mini, EDTA-free protease inhibitor mixture tab-

let/50 ml (Roche Diagnostics, Mannheim, Germany). Each tablet contained 3.0 mg of antipain HCl, 0.5 mg of bestatin, 1.0 mg of chymostatin, 3.0 mg of E-64, 0.5 mg of leupeptin, 0.5 of mg pepstatin, 3.0 mg of phosphoramidon, 20 mg of Pefabloc SC (Perspective Biosystems, Framingham, MA), 10 mg of ethylendiaminetetraacetic acid, and 0.5 mg of aproptinin. Cells were placed into a 15-ml glass homogenizer tube (three plates were combined for each data point), and the cells were homogenized by hand for 5 min. The lysate was centrifuged at 3000 $\times$ *g* for 5 min, the postnuclear fraction recovered and layer over 2 ml of 38% sucrose in 100 mM sodium carbonate. The samples were centrifuged in an ultracentrifuge at 25,000 rpm for 35 min, and the vesicle band was carefully recovered and transferred to a new ultracentrifuge tube. The tubes were filled with a 50 mM Tris solution containing 250 mM sucrose with added Complete Mini, EDTA-free protease inhibitor mixture tablets. The samples were again centrifuged in an ultracentrifuge at 26,000 rpm for 45 min to pellet the vesicles. Each pellet was resuspended in 100 ml of standard RIPA buffer [150 mM NaCl, 1% NP40, 0.5% deoxycholate, 0.1% SDS, and 50 mM Tris (pH 7.5)] and then prepared for analysis by inductively coupled plasma mass spectrometry as described above. For quantification, each sample was also analyzed for sulfur content using inductively coupled plasma optical emission spectroscopy (ICP-OES), and sulfur levels were used to normalize total Pt accumulation.

Western Blotting. Cells were rinsed twice with PBS, scraped from the dish in PBS, centrifuged for 10 min at 2500 rpm, and then lysed in 0.25% NP40 in 100 mM Tris HCl (pH 8.00) supplemented with 1 mM *p*-amidinophenyl methylsulfonyl fluoride hydrochloride and 1 mM γ-amino-n-caproic acid (Sigma Co.) at 4°C and for 30 min. Postnuclear fractions were obtained by centrifugation of cell lysates for 10 min at 600 $\times$ *g*. Samples containing 50–100 of μg protein were electrophoresed on 4–10% SDS polyacrylamide gels and then blotted onto nitrocellulose filters using a Bio-Rad Mini Transblot apparatus (Bio-Rad Co.). Blots were incubated for 1 h with 5% fat-free dry milk in Tris-buffered saline (TBS) at room temperature and then overnight in primary antibody against ATP7B from Dr. Jonathan D. Gitlin mixed with 5% milk in TBS at 4°C. Blots were washed three times for 15 min each at room temperature with 0.025% Tween 20 in TBS and then incubated with the secondary antibody dissolved in 5% fat-free dry milk in TBS for 1 h at room temperature. After three 15-min washes at room temperature in TBS with 0.025%, Tween 20 bands were visualized by chemiluminescence using the enhanced chemiluminescence kit from Amersham Biosciences on Fuji medical X-ray film (Super RX; Fujifilm, Kanagawa, Japan). A ChemiImager 4400 instrument (Alpha Inotech) was used for determining the relative density of protein bands.

Confocal Microscopy. Two cell lines, pECFP empty vector-transfected 2008 (2008/ECFP) and pECFP-ATP7B transfected cells (2008/ECFP-ATP7B), were used in these studies. Three days before staining, the cells were cultured on glass coverslips (Fisher Scientific Co.) in 24-well plates (Becton Dickinson, Franklin Lakes, NJ). After exposure to $CuSO_4$, DDP, F-DDP, or CHF, cells were washed three times with PBS and fixed with 3.7% formaldehyde in PBS. The cells were washed three times in PBS and then permeabilized in 0.3% Triton 100 in PBS for 15 min. Actin was stained with Alexa Fluor 647-conjugated phalloidin for 1 h using the manufacturer's protocol (Molecular Probes), after which, the coverslips were mounted on standard glass microscope slides. A confocal laser scanning microscope (ECLIPSE TE200; Nikon, Tokyo, Japan) was used to visualized the distribution of fluorescence at the UCSD Cancer Center Digital Imaging Shared Resource. Images were captured from 0.2-μm sections, and Soft Worx software (Applied Precision, Inc) on a Silicon Graphics Octane workstation was used for deconvoluting data. The effect of drug exposure on the subcellular localization of ECFP-ATP7B-expressing vesicles was quantified by measuring the distance, in arbitrary units, from the center of the nucleus to the three vesicles that were furthest from the nucleus in each of a panel of control and drug-treated cells. To account for variation in cell size, this distance was divided the product of the longest and shortest diameter of the nucleus divided by 2.

Evaluation of Colocalization between 2008/ECFP-ATP7B and CHF or F-DDP. The evaluation was performed using digital images of 2008/ECFP-ATP7B exposed to either CHF or F-DDP. The ECFP-ATP7B fusion protein was localized in vesicular structures that appeared as blue foci; CHF and F-DDP localized to vesicular structures that appeared green. Images were analyzed using Adobe Photoshop, version 6. The blue and green signal intensity was quantified in each pixel from 100 blue foci in images of 2008/ECFP-ATP7B cells exposed to either CHF or F-DDP.

Statistics. Tests of significance used Student's *t* test; *P* values of <0.05 were considered significant.

RESULTS

ATP7B Confers Resistance to Cu and DDP. These studies were carried out in sublines of the human ovarian carcinoma 2008 line that were transfected with either a vector that expressed ATP7B (2008/ATP7B cells) or just the empty vector alone (2008/EV cells). The effect of ATP7B expression on sensitivity to DDP and $CuSO_4$ was examined using an assay capable of detecting enrichment for ATP7B-expressing cells in the population that survived drug exposure. The 2008/ATP7B cells were further engineered to express GFP by infection with a viral vector expressing this protein. The 2008/EV and 2008/ATP7B-GFP cells were then mixed to form a population containing 10% 2008/ATP7B-GFP cells as determined before drug exposure by flow cytometric analysis. The mixed population was then exposed to increasing concentrations of DDP, carboplatin (CBDCA), oxaliplatin, or $CuSO_4$ for 1 h and then cultured for 5 days before the fraction of 2008/ATP7B-GFP cells was again determined by flow cytometry. The results of these experiments, presented in Fig. 1, demonstrated that in the absence of drug exposure, the fraction of 2008/ATP7B cells in the population did not change significantly during the 5 days of culture. However, all four compounds produced very substantial degrees of enrichment for ATP7B-expressing cells even at the lowest drug concentration tested. These results confirm our earlier studies that relied on clonogenic assays to document that increasing the level ATP7B expression in 2008 cells conferred a biologically important degree of resistance (37).

To study the subcellular localization of ATP7B, 2008 cells were transfected with either a vector that expressed ATP7B to

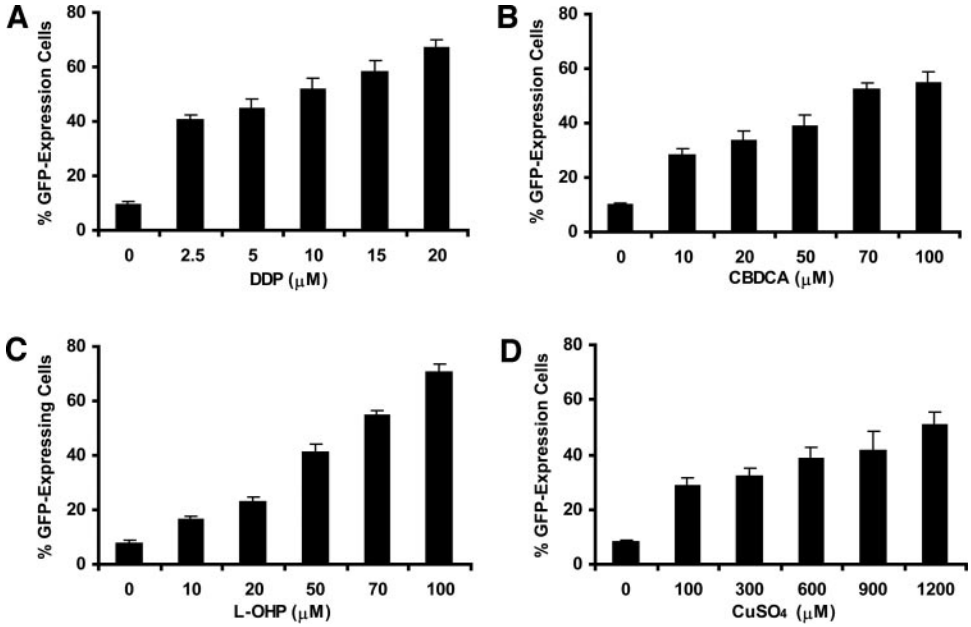

Fig. 1 Enrichment for cells expressing ATP7B after exposure to cisplatin (DDP), carboplatin (CBDCA), oxaliplatin (L-OHP), and Cu. The starting population contained 10% 2008/ATP7B-GFP-expressing cells and 90% 2008/EV. The cells were exposed to drug for 1 h, and the fraction of 2008/ATP7B-GFP-expressing cells in the surviving population was determined by flow cytometry 5 days later. *A*, DDP; *B*, CBDCA; *C*, L-OHP; *D*, $CuSO_4$. Each data point represents the mean of three experiments performed with duplicate cultures for each drug concentration. *Vertical bars*, ±SE. GFP, green fluorescent protein.

which enhanced cyan fluorescent protein (ECFP) was fused at the NH_2 terminus (2008/ECFPATP7B cells) or a control vector that expressed only ECFP (2008/ECFP cells). Both vectors also expressed a Geneticin resistance marker. After transfection, populations of cells that grew in the presence of Geneticin were tested by Western blotting for ATP7B expression using a polyclonal antibody directed at the NH_2-terminal sequences of the ATP7B protein. The ≈210 M_r ECFP-ATP7B fusion protein was present in the 2008/ECFP-ATP7B cells but was not detected in the control 2008/ECFP cells (data not shown). No endogenous ATP7B protein was detected in either cell type. Table 1 presents the IC_{50} values for each subline determined by clonogenic assay after a 1-h exposure to DDP or $CuSO_4$. On the basis of the IC_{50} values, the 2008/ECFP-ATP7B cells were 4.1-fold resistant to DDP and 1.9-fold resistant to $CuSO_4$ relative to the 2008/ECFP controls. These results establish that ATP7B expression produces a substantial degree of DDP resistance in this model and that the ECFP-ATP7B fusion protein is functionally competent.

Cu and DDP Accumulation. Studies of the accumulation of Cu and DDP were carried out in the 2008/ECFP and 2008/ECFP-ATP7B cells. Fig. 2, *A* and *B*, compares the cellular accumulation of Cu and DDP after 0.5, 1.0, or 1.5 h of drug exposure, respectively. For both Cu and DDP, the extent of accumulation was substantially less in the 2008/ECFP-ATP7B cells than in the 2008/ECFP cells at each time point ($P < 0.05$ for all comparisons). Thus, expression of ECFP-ATP7B reduced the accumulation of Cu and DDP in a parallel manner, confirming the results of earlier studies performed with native ATP7B (37) and additionally documenting the functionality of the ECFP-ATP7B fusion protein. Fig. 2*C* compares the accumulation of Pt in intracellular vesicles after 24 h of exposure to 2 μM DDP. The extent of accumulation of Pt in the vesicular fraction of the cell was 1.3-fold greater in the 2008/ECFP-ATP7B cells than in the 2008/ECFP cells ($P < 0.05$). Thus, although these preparations contain many kinds of vesicles other than just those expressing ATP7B, reduced whole-cell accumulation was associated with somewhat greater sequestration of DDP into the total mass of vesicular structures, some of which are likely to be components of the vesicular export pathway.

Table 1 IC_{50} for human ovarian cancer cell lines 2008/ECFP and 2008/ECFP-ATP7B exposed to DDP or $CuSO_4$ for 1 h[a]

	Cell line		
	2008/ECFP (μM, mean ± SD)	2008/ECFP-ATP7B (μM, mean ± SD)	*P*
DDP[b]	2.0 ± 0.4	8.1 ± 0.4	<0.001
$CuSO_4$	690.8 ± 47.3	1301.5 ± 18.1	<0.001

[a] ECFP, pECFP empty vector transfected; ECFP-ATP7B, pECFP-ATP7B cDNA transfected.
[b] DDP, cisplatin.

Subcellular Localization of ATP7B. A confocal laser scanning microscope tuned to detect fluorescence from ECFP was used to compare the subcellular localization of native ECFP in the 2008/ECFP cells with that of the ECFP-ATP7B fusion protein in the 2008/ECFP-ATP7B cells. Fig. 3 shows that, in the 2008/ECFP cells, fluorescence originating from the ECFP fluorophor was detected diffusely throughout the cytoplasm, whereas in the 2008/ECFP-ATP7B cells, the fluorescent signal was limited to structures clustered in the perinuclear region. This distribution of ECFP-ATP7B is consistent with the normal localization of ATP7B in the *trans*-Golgi network as demonstrated by prior studies in other cell systems (23, 27).

To examine the effect of drug exposure on the subcellular distribution of ATP7B, the 2008/ECFP-ATP7B cells were exposed to medium containing 200 μM $CuSO_4$ or 2 μM DDP for 1 h. As shown in Fig. 4, Cu triggered redistribution of ECFP-ATP7B from the perinuclear regions to more peripherally lo-

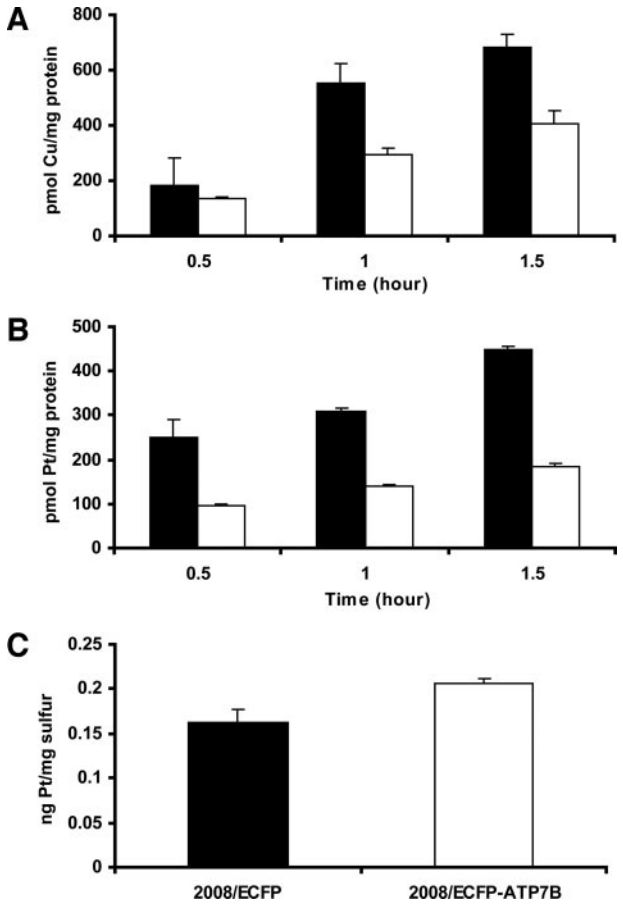

Fig. 2 Accumulation of Cu and cisplatin into whole cells and vesicles. *A* and *B* show accumulation of ^{64}Cu and Pt, respectively. *C* shows accumulation of Pt in vesicles isolated from 2008/ECFP-ATP7B and 2008/ECFP cells after a 24 h of exposure to 2 μM cisplatin. (■), 2008/ECFP cells; (□), 2008/ECFP-ATP7B cells. Each data point represents the mean of measurements made on six separate cultures/time point. *Vertical bars*, ±SE.

cated vesicles. This effect was quantified by examining the distance from the center of the nucleus to the three most peripheral ECFP-ATP7B-expressing vesicles in each of a panel of cells. This distance averaged 0.531 ± 0.017 (SE) in the control cells and 1.196 ± 0.063 in Cu-exposed cells ($P = 2.45 \times 10^{-6}$). This redistribution was evident by 1 h after the start of $CuSO_4$ exposure, and no additional progression was observed after 2 h of Cu exposure (data not shown). The images in Fig. 4 show that DDP also triggered redistribution of ECFP-ATP7B after 1 h [mean distance. 1.311 ± 0.046 (SE), $P = 1.90 \times 10^{-8}$]. Thus, a concentration of DDP within the range found in the plasma of patients receiving treatment with this drug triggered relocalization of ATP7B in a manner parallel to the effect produced by Cu itself. It is noteworthy that DDP produced this effect at a concentration 100 times lower than that of Cu.

Colocalization of ATP7B and F-DDP. If ECFP-ATP7B is in fact concentrating DDP into vesicles of the secretory pathway as it does Cu, then one might expect to find higher concentrations of DDP in vesicles that express ECFP-ATP7B than in other locations in the cell. To visualize the location of DDP, a fluorescein-conjugated form of DDP was synthesized. Fig. 5*A* shows the structures of F-DDP and of the fluorescent CHF molecule that lacks only the DDP moiety that was used as a control. Several studies were carried out to document that F-DDP was a valid mimic of DDP in these cells as it appears to be in other systems (34). F-DDP was compared with native DDP with respect to the magnitude of resistance in the well-studied isogenic pair of DDP-sensitive 2008 and DDP-resistant 2008/C13*5.25 cells. The results of clonogenic assays conducted with F-DDP and CHF are presented in Table 2. F-DDP was found to be 4-fold less potent than DDP against the 2008 cells, but the difference in sensitivity between the two cell lines was similar for F-DDP and DDP. The 2008/C13*5.25 cells were 5.7-fold more resistant to DDP than the 2008 cells (28) and were 5.5-fold more resistant to F-DDP. The fluorescein moiety itself, as contained in the CHF molecule, was not cytotoxic at concentrations up to 500 μM. These data indicate the mechanisms that protect 2008/C13*5.25 cells against DDP are also operative against F-DDP and suggest that the cytotoxicity of F-DDP is caused by the DDP moiety rather than the fluorescein label. 2008/C13*5.25 cells are known to have impaired cellular accumulation of DDP. To further validate F-DDP as a surrogate for DDP, cellular accumulation was determined in the 2008 and 2008/C13*5.25 cells by flow cytometry. The data presented in Fig. 5*B* show that accumulation of F-DDP was reduced in the 2008/C13*5.25 cells when measured at 0.5, 1.0, or 1.5 h after the start of F-DDP exposure ($P < 0.05$ for all time points). Thus, by this measure also, F-DDP behaves in a manner similar to that of DDP.

The images in Fig. 6 show that when the 2008/ECFP and 2008/ECFP-ATP7B cells were exposed to 2 μM CHF for 1 h, the pattern of CHF fluorescence was the same in both cell types, that there was little colocalization of CHF with either ECFP or ECFP-ATP7B, and that the ECFP-ATP7B remained in the perinuclear region in treated cells. Thus, expression of a functional ATP7B did not influence the intracellular localization of CHF, and CHF did not trigger the relocalization of ECFP-ATP7B [mean distance of vesicles furthest from nucleus, 0.574 ± 0.017 (SE), $P = 0.099$]. In contrast, the distribution of F-DDP was different in the 2008/ECFP and 2008/ECFP-ATP7B cells, indicating that expression of a functional ATP7B altered the localization of F-DDP. F-DDP at a concentration of 2 μM also dispersed the ECFPATP7B away from the perinuclear region [mean distance, 1.897 ± 0.124 (SE), $P = 3.25 \times 10^{-6}$].

This concentration of F-DDP had no effect on the distribution of ECFP in the 2008/ECFP cells. There was a substantial degree of colocalization between F-DDP and ECFP-ATP7B but not between F-DDP and ECFP. This demonstrates that, as with native DDP, the Pt-containing moiety in F-DDP remains functional with respect to its ability to induce a change in ATP7B distribution. The very high magnification images presented in Fig. 7*A* demonstrate that when 2008/ECFP-ATP7B cells were exposed to CHF, the CHF and ECFP-ATP7B resided largely in different vesicular compartments as evidenced by the lack of light blue color that depicts colocalization in the merged image. However, when they were exposed to F-DDP, there was extensive colocalization of the fluorescent signals from the F-DDP and ECFP-ATP7B. The extent of colocalization of the blue

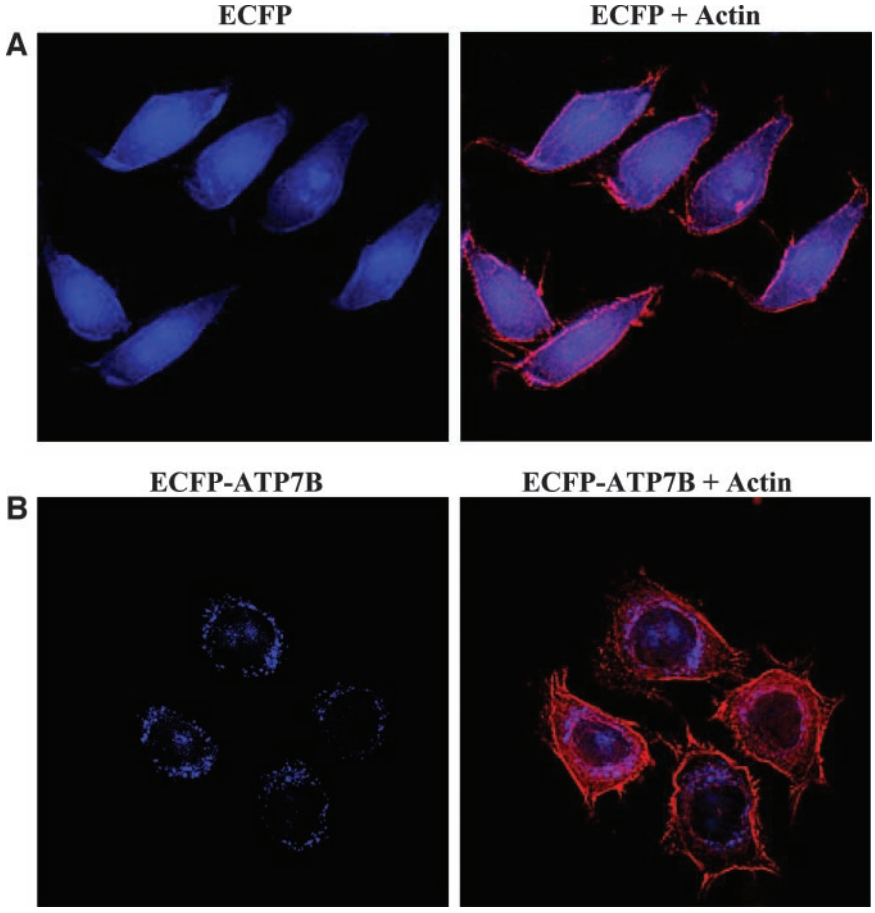

Fig. 3 Confocal microscopic images of the intracellular distribution of native enhanced cyan fluorescent protein (ECFP) *versus* ECFP-ATP7B fusion protein. *A*, distribution of ECFP in 2008/ECFP cells; *B*, distribution of ECFP-ATP7B in 2008/ECFP-ATP7B cells. Actin was stained with Alexa Fluor 647-conjugated phalloidin to facilitate identification of the cell margins. *Blue*, fluorescence from ECFP or ECFP-ATP7B; *red*, fluorescence from Alexa Fluor 647-conjugated phalloidin-stained actin.

signal from the ECFP-ATP7B and the green signal from either the CHF or F-DDP was quantified using image analysis software. Fig. 7*B* shows that green signal colocalized with blue signal when 2008/ECFP-ATP7B cells were exposed to F-DDP, whereas there was little colocalization when the cells were exposed to CHF. Thus, F-DDP, but not the control CHF molecule lacking only the DDP moiety, became concentrated into vesicles that express ATP7B. The extent of colocalization of the blue signal from the ECFP-ATP7B and the green signal from either the CHF or F-DDP was quantified using image analysis software. Fig. 7, *C* and *D*, shows that green signal colocalized with blue signal when 2008/ECFP-ATP7B cells were exposed to F-DDP, whereas there was little colocalization when the cells were exposed to CHF. Thus, F-DDP, but not the control CHF molecule lacking only the DDP moiety, became concentrated into vesicles that express ATP7B.

DISCUSSION

The observation that cells selected for DDP resistance are often cross-resistant to Cu and *vice versa* and that cellular accumulation of both DDP and Cu is impaired in both types of resistant cells (17) provides strong evidence that some component of the Cu homeostasis system regulates the responsiveness of cells to the Pt-containing drugs. Komatsu *et al.* (18) reported that increasing the expression of ATP7B in prostate cancer cells rendered them 8.9-fold resistant to DDP as quantified by inhibition of growth rate. Subsequent studies in our laboratory demonstrated that a small increase in the expression of ATP7B produced a more modest 1.6–2.6-fold resistance to DDP in three separate human ovarian carcinoma cells when measured using a clonogenic assay and showed that ATP7B also conferred resistance to CBDCA (28). The studies reported here extend and refine these observations further by showing that increased expression of ATP7B also confers resistance to oxaliplatin and that the magnitude of the resistance to all three Pt-containing drugs is sufficient to result in rapid enrichment of the population for ATP7B-expressing cells after drug exposure. The enrichment assays offer particularly cogent evidence of the significance of the degree of resistance conferred by ATP7B because both sensitive and resistant cells are exposed to exactly the same culture conditions throughout the assay (38). It is of interest that in all of the assay and cell systems studied thus far, ATP7B appears to render cells more resistant to DDP than to Cu (18, 37); the reason for this remains unknown.

Consistent with the ability of ATP7B to mediate resistance to Cu, our earlier studies demonstrated that Cu accumulation was reduced and efflux enhanced in 2008 cells engineered to express an increased level of ATP7B (28). ^{14}C-CBDCA accumulation and efflux were altered in a par-

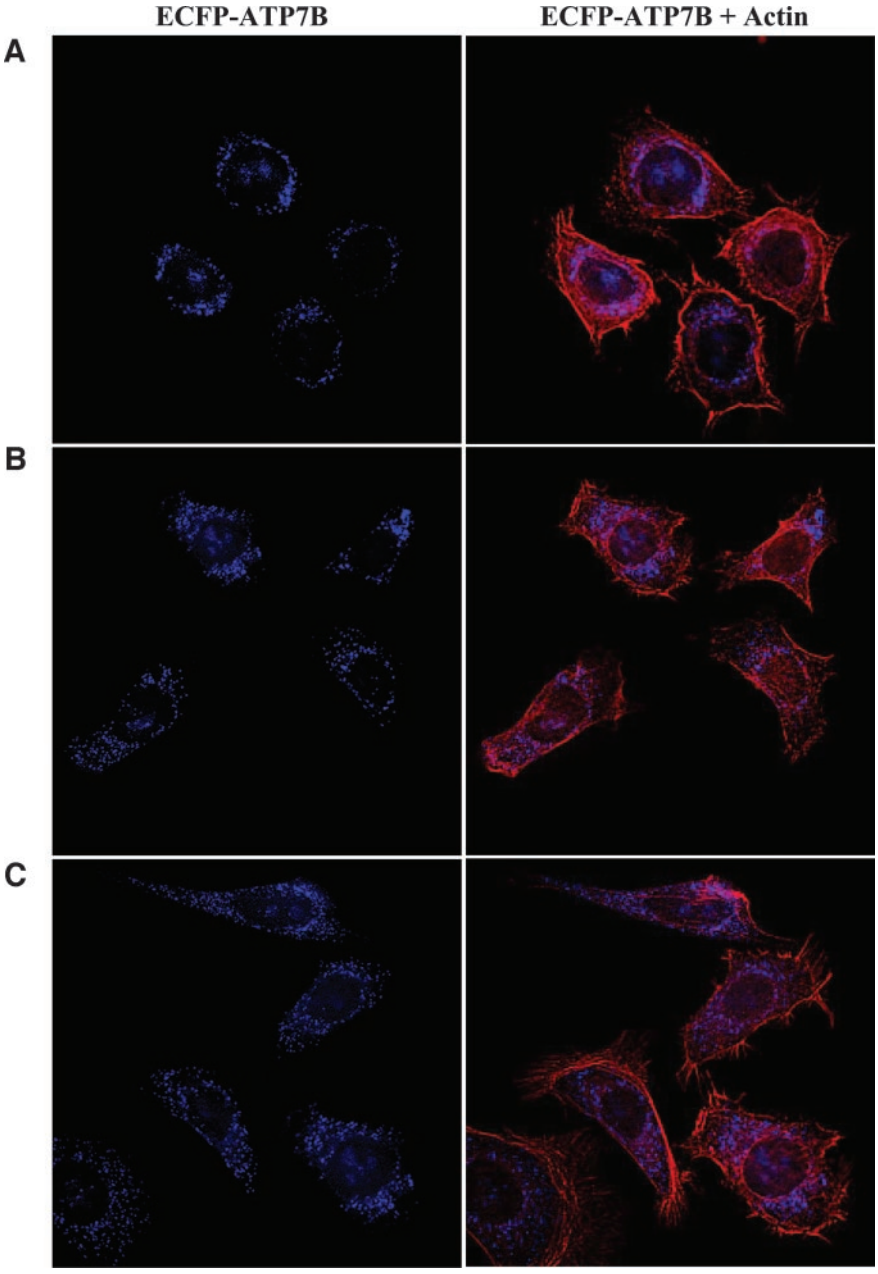

Fig. 4 Confocal microscopic images showing the effect of Cu and cisplatin on the intracellular distribution of ECFP-ATP7B in 2008/ECFP-ATP7B cells. *A*, no treatment; *B*, 200 μM $CuSO_4$ for 1 h; *C*, 2 μM cisplatin for 1 h. Colors are as identified in Fig. 3.

allel manner, suggesting that CBDCA is a substrate for the transport function of ATP7B. On the basis of the ability of ATP7B to confer resistance to DDP, we hypothesized that DDP is also a substrate for this transporter. To garner additional evidence for an interaction between DDP and ATP7B, in the current study, we engineered 2008 cells to express a fusion protein consisting of the cyan fluorescent protein ECFP and ATP7B. The ECFP-ATP7B fusion protein localized correctly to the perinuclear region as previously reported when cells are grown without addition of Cu to the medium (23, 25, 27, 39). The subcellular localization of ECFP-ATP7B also corresponded to the distribution of endogenous ATP7B under non-Cu-exposed conditions as reported by other investigators (30). The ECFP-ATP7B fusion protein appeared to be functional in that it conferred a degree of resistance to Cu and DDP that was actually higher, 1.9- and 4.1- fold, respectively, than that produced by expression of the native protein from the same type of vector, which was 1.2- and 2.6-fold, respectively (37). The ECFP-ATP7B fusion protein also reduced both the basal level of cellular Cu (data not shown) and the accumulation of Cu and DDP.

In the human ovarian cancer cell line used in this study, Cu altered the subcellular distribution of the ECFP-ATP7B fusion protein in a manner similar to that observed in other cell systems in which Cu triggers ATP7B trafficking (23, 25, 40, 41). DDP produced a very similar effect. This provides the most direct

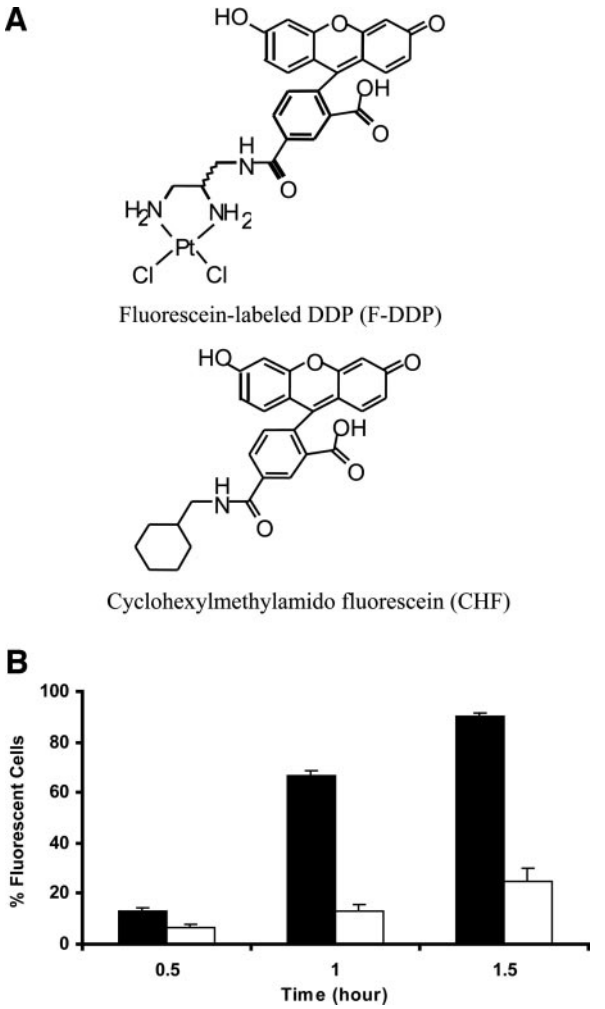

Fig. 5 Structures of fluorescein-labeled cisplatin (F-DDP) and cyclohexylmethylamido fluorescein (CHF) (*A*) and accumulation of F-DDP as a function of time determined by flow cytometry (*B*). (■), 2008 cells; (□), 2008/C13*5.25 cells. Each data point represents the mean of measurements made on three separate cultures/time point. *Vertical bars*, ±SE.

evidence currently available that DDP interacts with ATP7B. This is the first metalloid other than Cu that has been reported to cause the redistribution of ATP7B from the perinuclear region. Whether this reflects relocalization to a different type of vesicle or an alteration in the distribution of the vesicles in which the protein was originally located cannot be discerned from the data available. Using immobilized metal ion affinity chromatography, ATP7B has been shown to bind a variety of metalloids including Zn^{2+}, Hg^{2+}, Au^{3+}, and Cd^{2+} (42). However, no information is yet available as to whether or how DDP or the other Pt-containing drugs actually bind to ATP7B in whole cells.

Attempts to map the subcellular distribution of DDP in the cell using energy-dispersive X-ray microanalysis (43–45), electronic probes (46), or electron microscopy (47) have been hampered by the limited intracellular accumulation of the drug. Recently Molenaar *et al.* (34) described the synthesis of a fluorescein-labeled form of DDP and reported on its use for studying the cellular pharmacology of this drug. When one adds a fluorochrome to a small molecule, there is always the question of whether the labeled molecule has the same pharmacodynamics as the native drug. The results reported here provide evidence that it is the DDP moiety rather than the fluorescein in F-DDP that determines the cytotoxicity and intracellular fate of the drug and thus that its subcellular localization is a reasonable surrogate for the intracellular distribution of native DDP. The evidence is as follows. First, human ovarian carcinoma 2008/C13*5.25 cells selected for stable resistance to DDP were as cross-resistant to the cytotoxic effect of F-DDP as they were to DDP, indicating that F-DDP was subject to the same mechanisms that mediate resistance to the native drug. Second, whole-cell accumulation of both native DDP and F-DDP at 1 h was reduced to a similar extent in 2008/C13*5.25 cells. Third, the free fluorochrome moiety of F-DDP, CHF, had a completely different pattern of subcellular distribution than F-DDP and produced no cytotoxicity at concentrations up to 500 μM. Fourth, as with DDP, F-DDP triggered relocalization of ECFP-ATP7B. None of these points exclude the possibility that addition of fluorescein to DDP alters the cellular pharmacology of the drug in other ways, but they do provide evidence the DDP component causes F-DDP to retain many of the key characteristics of the native drug.

In cells expressing only ECFP, F-DDP was found in a variety of locations, including peripherally near the plasma membrane and in the nucleus, but it was most prominently concentrated into small vesicular structures scattered throughout the cytoplasm. Examination at both high and very high power disclosed little colocalization of F-DDP with ECFP in vesicular structures. On the other hand, in cells that expressed the ECFP-ATP7B fusion protein, there was quite extensive colocalization of F-DDP and the fusion protein in vesicular structures. This indicates that the vesicles that express the functional ECFP-ATP7B protein also contain F-DDP, consistent with the hypothesis that F-DDP is a substrate for ATP7B and is concentrated by this transporter into vesicular structures. That it is the DDP rather than the fluorescein that drives the ability of ATP7B to concentrate F-DDP in this manner is demonstrated by the fact that CHF itself showed a very different pattern of vesicular localization and showed no colocalization with ECFP-ATP7B.

The imaging data indicating the presence of F-DDP in

Table 2 Sensitivity of human ovarian cancer cell lines to a 1-h exposure to F-DDP and CHF[a]

	Cell line		
	2008 (μM, mean ± SD)	2008/C13*5.25 (μM, mean ± SD)	*P*
F-DDP	14.0 ± 0.7	76.3 ± 7.9	<0.01
CHF	[b]	[b]	
DDP	3.5 ± 0.4	20.1 ± 5.7	<0.05

[a] F-DDP, fluorescein-labeled form of cisplatin; CHF, cyclohexylmethylamido fluorescein; DDP, cisplatin.
[b] No cytotoxicity up to 500 μM.

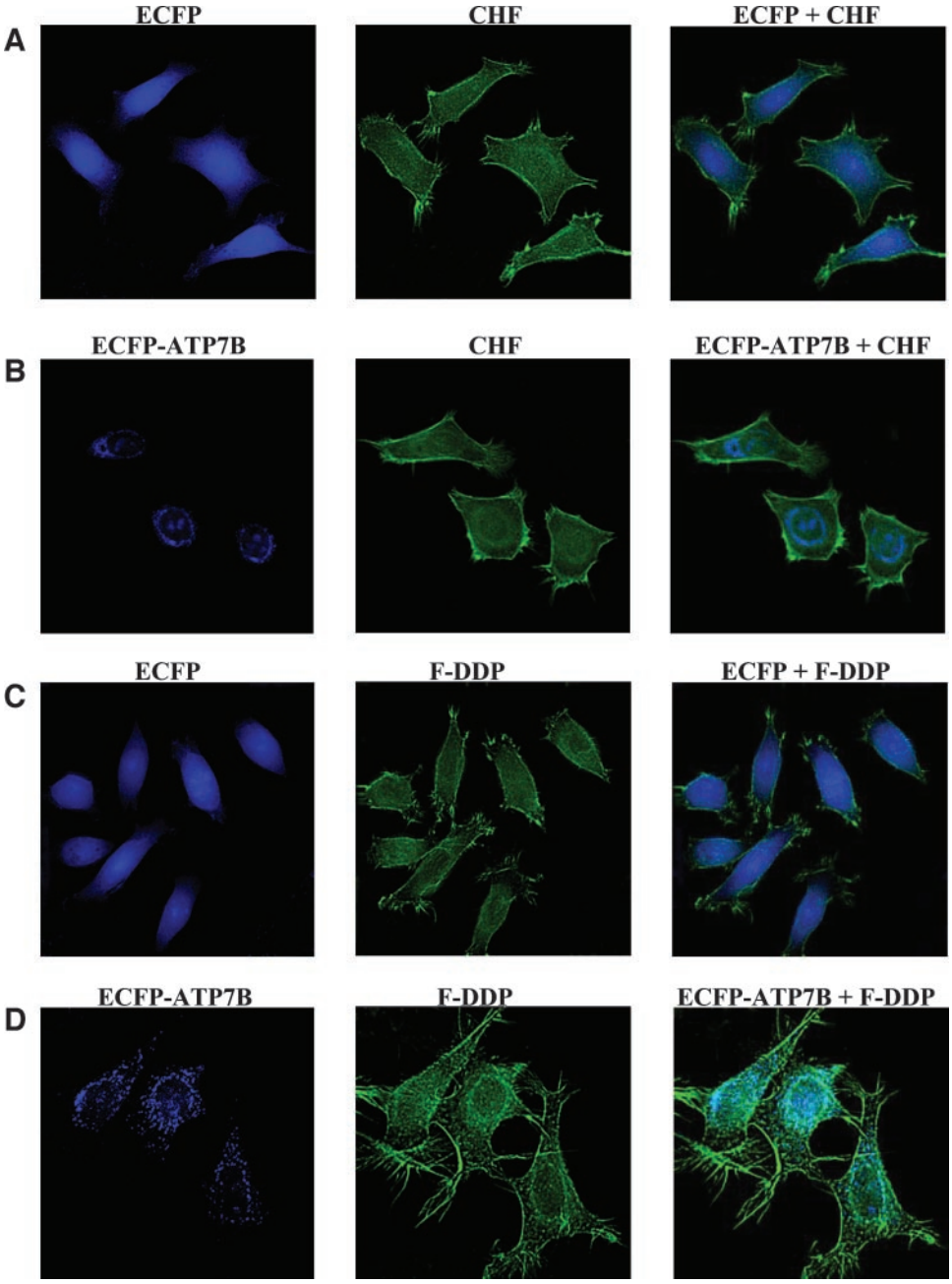

Fig. 6 Confocal microscopic images of the intracellular distribution of cyclohexylmethylamido fluorescein (CHF) and fluorescein-labeled cisplatin (F-DDP) in 2008/ECFP and 2008/ECFP-ATP7B cells. The *left panel* of each row shows the blue fluorescence from either enhanced cyan fluorescent protein (ECFP) or ECFP-ATP7B; the *middle panel* shows the green fluorescence from CHF or F-DDP; the *right panel* shows the merger of the *left* and *middle panels*. *A*, 2008/ECFP cells treated with 2 μM CHF for 1 h; *B*, 2008/ECFP-ATP7B cells treated with 2 μM CHF for 1 h; *C*, 2008/ECFP cells treated with 2 μM F-DDP for 1 h; *D*, 2008/ECFP-ATP7B cells treated with 2 μM F-DDP for 1 h. *Green*, fluorescence from CHF or F-DDP; *blue*, fluorescence from ECFP or ECFP-ATP7B.

close association with ATP7B in vesicular structures is consistent with the finding that the 2008/ECFP-ATP7B cells sequestered more Pt into vesicular structures than the 2008/ECFP cells as measured by inductively coupled plasma mass spectrometry. As it was not possible to isolate vesicles expressing ATP7B from all other vesicles in the cells, a rigorous mass balance of Pt in various compartments of the cell could not be done, and it remains unknown what fraction of the intracellular drug is found in vesicles at any particular time point during drug exposure. However, taken together, these observations suggest that ATP7B, rather than pumping DDP out of the cell at the plasma membrane, functions to enhance DDP efflux by sequestering it into the vesicular export pathway that is known to efficiently export Cu. It is important to note that it has not yet been demonstrated in a well-defined system that DDP, CBDCA, or oxaliplatin are actually substrates for the ATP7B transporter. Likewise, although some cell lines selected for resistance to DDP overexpress ATP7B, it is not known whether the ATP7B is the direct cause of the resistance. Nevertheless, the available evidence is consistent with the hypothesis that this Cu transporter is able to limit the cytotoxicity of the Pt drugs by sequestering it into vesicles that are subsequently exported from the cell.

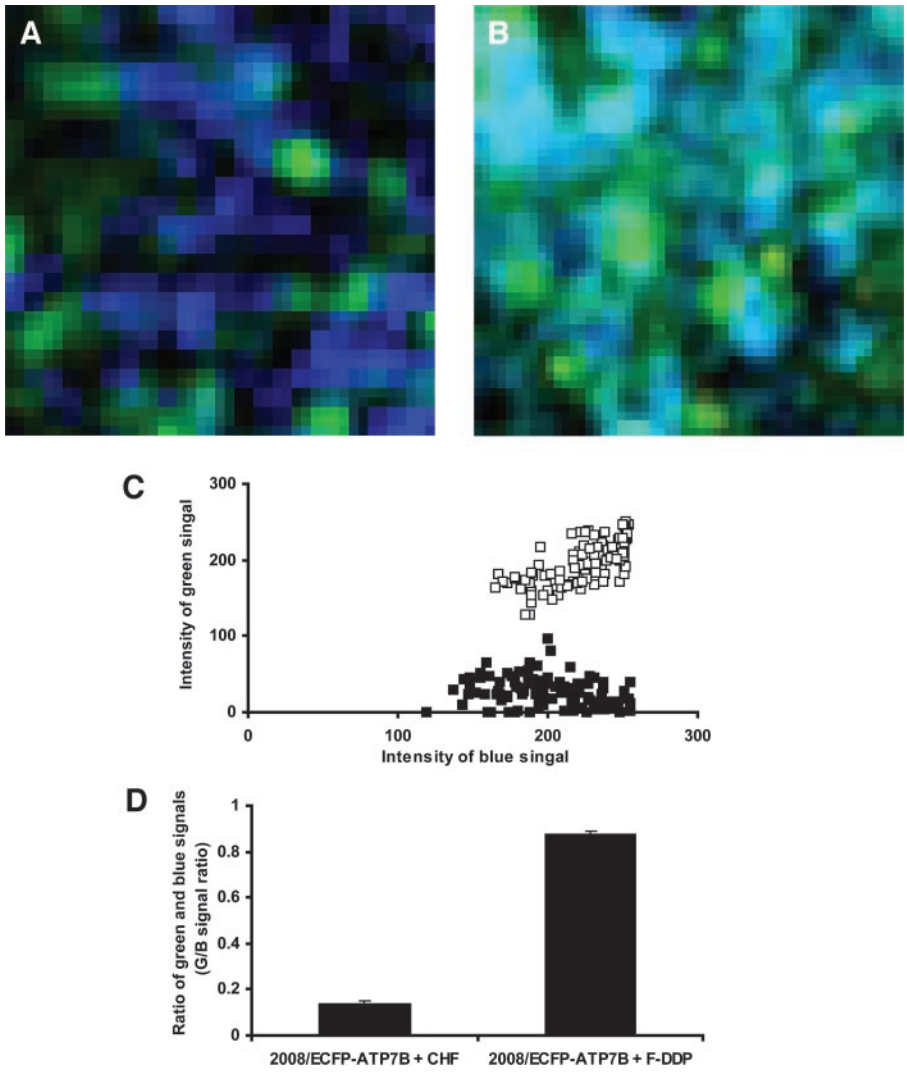

Fig. 7 Colocalization of fluorescein-labeled cisplatin (F-DDP) with ECFP-ATP7B. *A*, 2008/ECFP-ATP7B cells exposed to cyclohexylmethylamido fluorescein (CHF); *B*, 2008/ECFP-ATP7B cells exposed to F-DDP. *Green*, fluorescence from CHF or F-DDP; *blue*, fluorescence from ECFP-ATP7B. *Light blue* indicates colocalization. *C*, analysis of colocalization between blue and green signals in the images shown in *A* and *B*. One-hundred blue or light blue dots in each picture were selected, and signal intensity of blue signal and green signal in blue or light blue dots was evaluated. The figure shows the relative blue (ECFP-ATP7B) and green (CHF or F-DDP) signal intensity from each of 100 blue vesicular structures in 2008/ECFP-ATP7B cells exposed to CHF (■) or F-DDP (□). *D*, mean green to blue signal intensity in blue vesicular structures. *Vertical bars*, ±SE.

ACKNOWLEDGMENTS

We thank Drs. Toshihiro Sugiyama, Michael Petris, and Jonathan D. Gitlin and Martin Haas for providing essential vectors and reagents, Dr. James Feramisco for assistance with confocal imaging, Wiltrud Naerdemann for excellent technical assistance, and Claudette Zacharia for project management assistance.

REFERENCES

1. Andrews, PA. Mechanisms of acquired resistance to cisplatin. In: Ozols RF, Goldstein LJ, editors. Drug resistance. Boston: Kluwer Academic; 1994. p. 217–48.

2. Akiyama S, Chen ZS, Sumizawa T, Furukawa T. Resistance to cisplatin. Anticancer Drug Res 1999;14:143–51.

3. Hinoshita E, Uchiumi T, Taguchi K, et al. Increased expression of an ATP-binding cassette superfamily transporter, multidrug resistance protein 2, in human colorectal carcinomas. Clin Cancer Res 2000;6:2401–7.

4. Gately DP, Howell SB. Cellular accumulation of the anticancer agent cisplatin: a review. Br J Cancer 1993;67:1171–6.

5. Waud WR. Differential uptake of *cis*-diamminedichloro-platinum(II) in sensitive and resistant murine L1210 leukemia cell lines. Cancer Res 1987;46:6549–55.

6. Teicher BA, Holden SA, Herman TS, et al. Characteristics of five human tumor cell lines and sublines resistant to *cis*-diamminedichloroplatinum(II). Int J Cancer 1991;47:252–60.

7. Oldenburg J, Begg AC, van Vugt MJH, et al. Characterization of resistance mechanisms to *cis*-diamminedichloroplatinum (II) in three sublines of the CC531 colon adenocarcinoma cell line *in vitro*. Cancer Res 1994;54:487–93.

8. Twentyman PR, Wright KA, Mistry P, Kelland LR, Murrer BA. Sensitivity to novel platinum compounds of panels of human lung cancer cell lines with acquired and inherent resistance to cisplatin. Cancer Res 1992;52:5674–80.

9. Andrews PA, Albright KD. Role of membrane ion transport in cisplatin accumulation. In: Howell SB, editor. Platinum and other metal coordination compounds in cancer chemotherapy. New York: Plenum Press; 1991. p. 151–9.

10. Andrews PA, Mann SC, Huynh HH, Albright KD. Role of the Na+, K+ATPase in the accumulation of *cis*-diammine-dichloroplatinum(II) in human ovarian carcinoma cells. Cancer Res 1991;51:3677–81.

11. Andrews PA, Velury S, Mann SC, Howell SB. *cis*-diamminedichloroplatinum(II) accumulation in sensitive and resistant human ovarian carcinoma cells. Cancer Res 1988;48:68–73.

12. Mann SC, Andrews PA, Howell SB. Modulation of *cis*-diamminedichloroplatinum(II) accumulation and sensitivity by forskolin and 3-isobutyl-1-methylxanthine in sensitive and resistant human ovarian carcinoma cells. Int J Cancer 1991;48:866–72.

13. Mann SC, Andrews PA, Howell SB. Short-term *cis*-diamminedichloroplatinum (II) accumulation in sensitive and resistant human ovarian carcinoma cells. Cancer Chemother Pharmacol 1990;25:236–40.

14. Chau Q, Stewart DJ. Cisplatin efflux, binding and intracellular pH in the HTB56 human lung adenocarcinoma cell line and the E-8/0.7 cisplatin-resistant variant. Cancer Chemother Pharmacol 1999;44:193–202.

15. Ishikawa T, Wright CD, Ishizuka, H. GS-X pump is functionally overexpressed in *cis*-diamminedichloroplatinum(II)-resistant human leukemia HL-60 cells and down-regulated by cell differentiation. J Biol Chem 1994;269:29085–93.

16. Ishikawa T, Ali-Osman F. Glutathione-associated *cis*-diamminedichloroplatinum(II) metabolism and ATP-dependent efflux from leukemia cells. J Biol Chem 1993;268:20116–25.

17. Safaei R, Katano K, Samimi G, et al. Cross-resistance to cisplatin in cells with acquired resistance to copper. Cancer Chemother Pharmacol 2004;53:239–46.

18. Komatsu M, Sumizawa T, Mutoh M, et al. Copper-transporting P-type adenosine triphosphatase (ATP7B) is associated with cisplatin resistance. Cancer Res 2000;60:1312–6.

19. Bull PC, Thomas GR, Rommens JM, Forbes JR, Cox DW. The Wilson disease gene is a putative copper transporting P-type ATPase similar to the Menkes gene. Nat Genet 1993;5:327–37.

20. Tanzi RE, Petrukhin K, Chernov I, et al. The Wilson disease gene is a copper transporting ATPase with homology to the Menkes disease gene. Nat Genet 1993;5:344–50.

21. Yamaguchi Y, Heiny ME, Gitlin JD. Isolation and characterization of a human liver cDNA as a candidate gene for Wilson's disease. Biochem Biophys Res Commun 1993;197:271–7.

22. Tao TY, Gitlin JD. Hepatic copper metabolism: insights from genetic disease. Hepatology 2003;37:1241–7.

23. Roelofsen H, Wolters H, Van Luyn MJ, Miura N, Kuipers F, Vonk RJ. Copper-induced apical trafficking of ATP7B in polarized hepatoma cells provides a mechanism for biliary copper excretion. Gastroenterology 2000;119:782–93.

24. Harada M, Kumemura H, Sakisaka S, et al. Wilson disease protein ATP7B is localized in the late endosomes in a polarized human hepatocyte cell line. Int J Mol Med 2003;11:293–8.

25. Hung IH, Suzuki M, Yamaguchi Y, Yuan DS, Klausner RD, Gitlin JD. Biochemical characterization of the Wilson disease protein and functional expression in the yeast *Saccharomyces cerevisiae.* J. Biol Chem 1997;272:21461–6.

26. Vanderwerf SM, Cooper MJ, Stetsenko IV, Lutsenko S. Copper specifically regulates intracellular phosphorylation of the Wilson's disease protein, a human copper-transporting ATPase. J Biol Chem 2001; 276:36289–94.

27. Schaefer M, Roelofsen H, Wolters H, et al. Localization of the Wilson's disease protein in human liver. Gastroenterology 1999;117: 1380–5.

28. Katano K, Kondo A, Safaei R, et al. Acquisition of resistance to cisplatin is accompanied by changes in the cellular pharmacology of copper. Cancer Res 2002;62:6559–65.

29. Disaia PJ, Sinkovics JG, Rutledge FN, Smith JP. Cell-mediated immunity to human malignant cells. Am J Obstet Gynecol 1972;114: 979–89.

30. Harada M, Sakisaka S, Kawaguchi T, et al. Copper does not alter the intracellular distribution of ATP7B, a copper-transporting ATPase. Biochem Biophys Res Commun 2000;275:871–6.

31. Terada K, Nakako T, Yang X-L, et al. Restoration of holoceruloplasmin synthesis in LEC rat after infusion of recombinant adenovirus bearing WND cDNA. J Biol Chem 1998;273:1815–20.

32. Norris PS, Jepsen K, Haas M. High-titer MSCV-based retrovirus generated in the pCL acute virus packaging system confers sustained gene expression *in vivo*. J Virol Methods 1998;75:161–7.

33. Fink D, Nebel S, Norris PS, et al. Enrichment of DNA mismatch repair-deficient cells during treatment with cisplatin. Int J Cancer 1998; 77:741–6.

34. Molenaar C, Teuben JM, Heetebrij RJ, Tanke HJ, Reedijk J. New insights in the cellular processing of platinum antitumor compounds, using fluorophore-labeled platinum complexes and digital fluorescence microscopy. J Biol Inorganic Chem 2000;5:655–65.

35. Lee J, Petris MJ, Thiele DJ. Characterization of mouse embryonic cells deficient in the Ctr1 high affinity copper transporter. J Biol Chem 2002;277:40253–9.

36. Shen DW, Goldenberg S, Pastan I, Gottesman MM. Decreased accumulation of [^{14}C] carboplatin in human cisplatin-resistant cells results from reduced energy-dependent uptake. J Cell Physiol 2000;183: 108–16.

37. Katano K, Safaei R, Samimi G, Holzer A, Rochdi M, Howell SB. The copper export pump ATP7B modulates the cellular pharmacology of carboplatin in ovarian carcinoma cells. Mol Pharmacol 2003;64:466–73.

38. Torrance CJ, Agrawal V, Vogelstein B, Kinzler KW. Use of isogenic human cancer cells for high-throughput screening and drug discovery. Nat Biotechnol 2001;19:940–5.

39. Yang X-L, Miura N, Kawarada Y, et al. Two forms of Wilson disease protein produced by alternative splicing are localized in distinct cellular compartments. Biochem J 1997;326:897–902.

40. Payne AS, Kelly EJ, Gitlin JD. Functional expression of the Wilson disease protein reveals mislocalization and impaired copper-dependent trafficking of the common H1069Q mutation. Proc Natl Acad Sci USA 1998;95:10854–9.

41. Schaefer M, Hopkins RG, Failla ML, Gitlin JD. Hepatocyte-specific localization and copper-dependent trafficking of the Wilson's disease protein in the liver. Am J Physiol 1999;276:G639–46.

42. DiDonato M, Narindrasorasak S, Forbes JR, Cox DW, Sarkar B. Expression, purification, and metal binding properties of the N-terminal domain from the Wilson disease putative copper-transporting ATPase (ATP7B). J Biol Chem 1997;272:33279–82.

43. Berry JP, Galle P, Viron A, Kacerovska H, Macieira-Coelho A. Preferential nucleolar localization of *cis*-DDP in human fibroblasts. Biomed Pharmacother 1983;37:125–9.

44. Makita T, Hakoi K, Ohokawa T. X-ray microanalysis and electron microscopy of platinum complex in the epithelium of proximal renal tubules of the cisplatin administered rabbits. Cell Biol Int Rep 1986;10: 447–54.

45. Makita T, Itagaki S, Ohokawa T. X-ray microanalysis and ultrastructural localization of cisplatin in liver and kidney of the rat. Jpn J Cancer Res 1985;76:895–901.

46. Berry JP, Brille P, LeRoy AF, et al. Experimental ultrastructural and X-ray microanalysis study of cisplatin in the rat: intracellular localization of platinum. Cancer Treat Rep 1982;66:1529–33.

47. Meijera C, van Luyn MJ, Nienhuis EF, Blom N, Mulder NH, de Vries EG. Ultrastructural morphology and localization of cisplatin-induced platinum-DNA adducts in a cisplatin-sensitive and -resistant human small cell lung cancer cell line using electron microscopy. Biochem Pharmacol 2001;61:573–8.